



**HAL**  
open science

## Calcium alumino-silicates hydrates (C-A-S-H) carbonation kinetics

Ekoé Kangni-Foli, Stéphane Poyet, Patrick Le Bescop, Thibault Charpentier, Alexandre Dauzeres, Emilie L'Hopital, Jean-Baptiste D'espinoze de Lacaille

► **To cite this version:**

Ekoé Kangni-Foli, Stéphane Poyet, Patrick Le Bescop, Thibault Charpentier, Alexandre Dauzeres, et al.. Calcium alumino-silicates hydrates (C-A-S-H) carbonation kinetics. ICCC 2019 - 15th International Congress on the Chemistry of Cement, Sep 2019, Prague, Czech Republic. cea-03211966

**HAL Id: cea-03211966**

**<https://cea.hal.science/cea-03211966>**

Submitted on 29 Apr 2021

**HAL** is a multi-disciplinary open access archive for the deposit and dissemination of scientific research documents, whether they are published or not. The documents may come from teaching and research institutions in France or abroad, or from public or private research centers.

L'archive ouverte pluridisciplinaire **HAL**, est destinée au dépôt et à la diffusion de documents scientifiques de niveau recherche, publiés ou non, émanant des établissements d'enseignement et de recherche français ou étrangers, des laboratoires publics ou privés.

# Calcium alumino-silicates hydrates (C-A-S-H) carbonation kinetics

Kangni-Foli E. <sup>1,2</sup>, Poyet S. <sup>3</sup>, Le Bescop P. <sup>3</sup>, Charpentier T. <sup>4</sup>, Dauzères A. <sup>1</sup>, L'Hôpital E. <sup>1</sup>, d'Espinose de Lacaillerie J.-B. <sup>2</sup>

(1) IRSN, Institute of Radiation Protection and Nuclear Safety, PSE-ENV/SEDRE/ LETIS, BP 17, F-92262 Fontenay Aux Roses, France

(2) Soft Matter Science and Engineering, UMR CNRS 7615, ESPCI Paris, Université PSL, 10 rue Vauquelin, 75005 Paris, France

(3) Den-Service d'Etude du Comportement des Radionucléides (SECR), CEA, Université de Paris-Saclay, F-91191 Gif-sur-Yvette cedex, France

(4) NIMBE, CEA, CNRS, Université Paris-Saclay, CEA Saclay, F-91191 Gif-sur-Yvette Cedex, France

## 1. ABSTRACT

In this study, we intended to characterize the impact of carbonation on the main cement hydrate (C-A-S-H) in terms of chemistry and kinetics of degradation as well as to provide a better understanding on the carbonation products' properties. We synthesized C-A-S-H with increasing calcium content, *i.e.* Ca/Si ratios ranging from 0.80 to 1.40 and Al/Si ratios of 0.05 and 0.10. Based on thermogravimetric, <sup>27</sup>Al and <sup>29</sup>Si magic angle spinning nuclear magnetic resonance and x-ray diffraction preliminary results, it was observed that C-A-S-H and C-S-H generated, after carbonation, the same major and minor calcium carbonates polymorphs (vaterite and aragonite, respectively) and the same amorphous product (silica gel). For the C-S-H, the silica gel embedded the fraction of calcium not transformed in calcium carbonate and, it was also the case for C-A-S-H silica gel which incorporates also aluminium. It was also found that coupling a high aluminium content with a high calcium content, *i.e.* Ca/Si higher than 0.95, calcium aluminates hydrates of pentahedral and octahedral coordination (third aluminate hydrate, TAH) are produced. The pentahedral product is located in the C-A-S-H interlayers and the TAH on its surfaces. The presence of those species correlated with a lower kinetic of degradation for the C-A-S-Hs. A proper understanding of the mechanisms involved requires further studies but from these preliminary results, the hypothesis of a CO<sub>2</sub> access to the C-A-S-H limited by the calcium aluminates with Al in pentahedral environment and TAH seems acceptable

## 2. INTRODUCTION

Extensive studies on cementitious materials carbonation [1,2,11–18,3–10] have been released these last years and the topic is still the concern of ongoing studies. This is explained by the extent of the alteration that could originate from the carbonation and its consequences on the materials durability (carbonation mainly provides the conditions for active corrosion of steel reinforcement). Despite being extensively studied, several aspects such as the kinetics of carbonation and the properties of the products of carbonation remain partially understood. In this study we synthesized C(-A)-S-Hs of (increasing) Ca to Si ratios (C/S) comprised between 0.80 and 1.40 at two Al to Si ratios 0.05 and 0.1. These samples were submitted to accelerated (P<sub>CO2</sub>= 3%) and natural carbonation (P<sub>CO2</sub>= 0.04%). The representativeness between the two types of carbonation was assessed as well as the progress of the carbonation and the mechanisms involved. We focused on the consequences of carbonation at the molecular scale, by investigating the nature of the product yielded by C(-A)-S-Hs' ultimate state of carbonation and the influence of Al on the carbonation kinetics.

## 3. MATERIALS AND METHODS

### 3.1 Samples

C(-A)-S-Hs were synthesized in ultrapure water (Milli-Q) using CaO (provided by Alfa Aesar), silica Aerosil 200 (from Evonik industries) and CaOAl<sub>2</sub>O<sub>3</sub> (sourced by Alfa Aesar). A water/solid ratio of 50 was used for all syntheses. The C-A-S-H were obtained through one step synthesis by mixing the stoichiometric amount of powders (Table 1) in HDPE bottles. The bottles were rotated at 15 rpm and kept at 22 °C ± 2 °C during 6 months.

**Table 1: composition of the C-A-S-H that were synthesized**

Target C/S	0.80			0.95			1.20			1.40		
Target Al/Si	0.00	0.05	0.10	0.00	0.05	0.10	0.00	0.05	0.10	0.00	0.05	0.10

After that, the solutions were filtrated and the resulting products were dried at ambient temperature. Please note that all these operations were conducted in a CO<sub>2</sub>-free glovebox to prevent parasitic carbonation.

### 3.2 Methods

Thermogravimetric analyses (TGA) data were acquired on a Netzsch STA 409 PC Luxx apparatus. Analyses were ran under constant N<sub>2</sub> flowing (80 ml/min) and a heating rate of 10 °C/min. The weight losses from samples of 120 mg of powder were recorded from 25 °C to 1150 °C. Quantification were based on weight losses due to calcium carbonate decompositions.

C-A-S-Hs' mineralogical properties were unveiled by powder X-ray diffraction (XRD). Data were collected on a XPD PANalytical X'Pert diffractometer with a Bragg-Brentano geometry,  $\Theta$ - $\Theta$  configuration, and using Cu K $\alpha$  radiation as a light source operated at 45 kV and 40 mA.

Silicon and aluminium magic-angle spinning nuclear magnetic resonance (<sup>29</sup>Si and <sup>27</sup>Al MAS NMR) single-pulse data were collected at ambient temperature, using a Bruker Avance III 500 spectrometer operating at a Larmor frequency resonance of 99.3 MHz and 130.06 MHz respectively. Conditions were set to a  $\pi/2$  pulses of 3.5  $\mu$ s, a recycle delays of 20 s, a 7 mm zirconia rotor spinning at 5.5 kHz and a minimum number of 4000 scans for each <sup>29</sup>Si spectrum. For <sup>27</sup>Al analyses, a 1  $\mu$ s  $\pi/6$  pulse and a recycle delay between 1 s and 2 s was retained. A 4 mm zirconia rotor was spun at 12.5 kHz and a minimum number of 4000 scans were acquired. Tetramethylsilane and AlCl<sub>3</sub> aqueous solutions were used as an external standard to report the chemical shifts for <sup>29</sup>Si and <sup>27</sup>Al respectively. NMR data were processed using an internally developed software [19]. The Tobermoritic structure model was adopted, which implies for the C(-A)-S-Hs chains based on the dreierketten pattern: paired tetrahedra noted Q<sup>2p</sup> forming dimers and linked by a third tetrahedron noted Q<sup>2b</sup> thus forming the dreierketten pattern. The Tobermoritic structure model was applied by defining the number of bridging tetrahedra (Q<sup>2b</sup>) as half of the population of the pairing tetrahedra (Q<sup>2p</sup>) *i.e.*:  $Q^{2p} = 2Q^{2b}$ .

The natural and the accelerated powders' carbonation were implemented using climatic chambers at 25 °C, relative humidity of 55%, P<sub>CO2</sub> of 0.04% and 3% respectively.

## 4. RESULTS

For the C-S-H (*i.e.* C-A-S-H with the Al/Si ratio of 0), the <sup>29</sup>Si MAS-NMR spectra showed two main types of environment: silicates tetrahedra connected either to one tetrahedron (Q<sup>1</sup>) or two tetrahedra (Q<sup>2p</sup>, Q<sup>2b</sup>) (Figure 1). An increase of the coordination of the silicates tetrahedra was observed with the decrease of the C/S ratio. A decrease of the C/S ratio led to a predominance of Q<sup>2</sup> environments as expected from numerous previous studies, see for example [20–22]. The C-A-S-H <sup>29</sup>Si MAS-NMR spectra (Figure 2 and Figure 3) exhibited the same type of silicates environment (mainly Q<sup>1</sup>, Q<sup>2p</sup>, Q<sup>2b</sup>) as C-S-H but with broader resonances. This was believed to arise: (1) firstly from Q<sup>n</sup>(mAl) environments (silicates tetrahedra connected to m tetrahedral aluminium) as resulting from the substitution of silicates tetrahedra by aluminium tetrahedra [23–25]) and, (2) from the disorder generated by the presence of Al which led to a larger distribution of the chemical shifts. For a given C/S, an increase in the relative proportion of silicates with higher coordination number (Q<sup>2p</sup>, Q<sup>2b</sup>) [26] was noticed when the aluminium content increased (Figure 1, Figure 2, Figure 3).

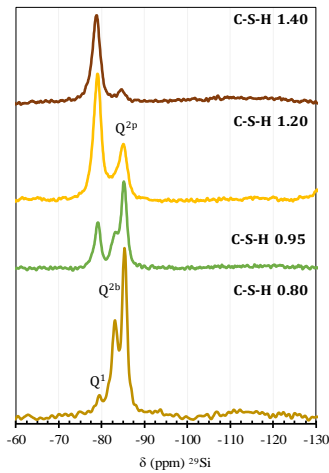


**Figure 1:  $^{29}\text{Si}$  MAS NMR spectra of the C-S-H**

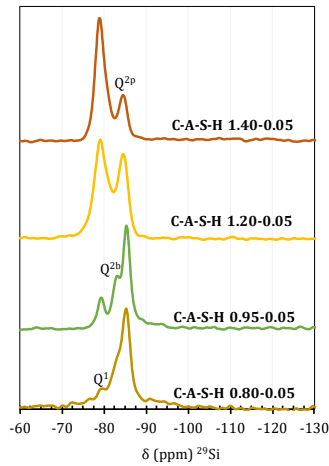


**Figure 2:  $^{29}\text{Si}$  MAS NMR spectra of C-A-S-H Al/Si = 0.05**

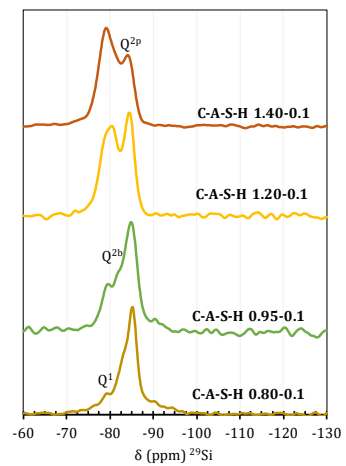


**Figure 3:  $^{29}\text{Si}$  MAS NMR spectra of C-A-S-H Al/Si = 0.10**

The  $^{27}\text{Al}$  MAS-NMR spectra are presented on Figure 4. One can see the variation induced by both the C/S ratios and the Al content on C-A-S-H's Al environments. C-A-S-Hs of low C/S ratios (0.80 and 0.95) mainly exhibited Al resonances in agreement with tetrahedral (50-80 ppm) and octahedral (0-20 ppm) environments, as previously observed [27–29]. Occurrence of Al in pentahedral coordination ( $\approx 35$  ppm) correlated with an increase of the calcium content, noticeable in the spectra of the samples with a C/S ratio of 0.95 to 1.40. However, the relative proportion of Al pentahedral resonance at C/S= 0.95 barely exceeds 5% of the total  $^{27}\text{Al}$  NMR signal intensity, for all Al contents (0.05 and 0.1), see Table 2. At higher C/S ratios (1.20 and 1.40), the three coordinations of Al were observed namely tetrahedral, pentahedral and octahedral. The increase of the calcium content from the C/S ratio 0.95 to 1.2 induced either an increase of the proportion of the pentahedral environment and a strong change in octahedral environments. A second type of octahedral environment called the third aluminate hydrate (TAH) appeared (0-5 ppm). The proportion of TAH increased from traces at C/S= 0.80 and 0.95 to reach 45% of the total Al environments at C/S = 1.40 Al/Si = 0.10 (Table 2). The second type of Al octahedral environment is attributed to species such as calcium aluminium hydrates [27,28,30]; phases that were not associated to C-A-S-H [31] (noted Al h in Table 2).

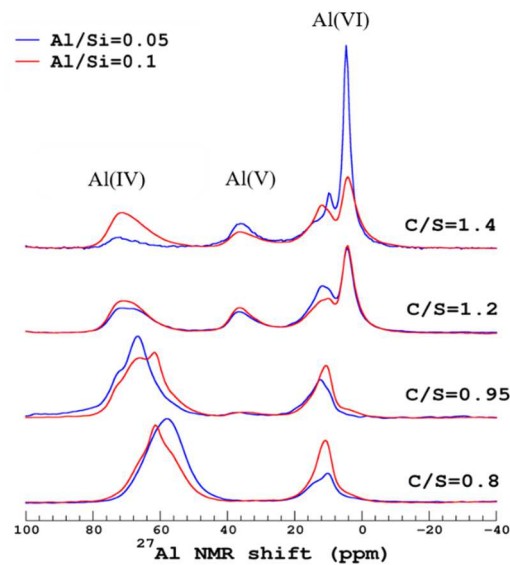


**Figure 4:  $^{27}\text{Al}$  MAS-NMR of the C-A-S-Hs**

**Table 2: Properties and distribution of C-A-S-Hs  $^{27}\text{Al}$  signal intensities, Al h refers to calcium**

aluminates hydrates such as C2AH8, C4AH13-19

Target C/S–Al/Si	Al/Si (from <sup>27</sup> Al NMR)	% Al incorporated in C-S-H as Al(IV)	%Al (V)	%Al (VI)	
				%Al h	%TAH
0.80-0.05	0.038	75	0	25	≈ 0
0.95-0.05	0.032	64	5.2	30.8	≈ 0
1.20-0.05	0.013	26.7	14.3	35	24
1.40-0.05	0.017	34.3	11.5	31	23.2
0.80-0.10	0.059	59.1	0	40.9	≈ 0
0.95-0.10	0.062	61.6	5.0	33.4	≈ 0
1.20-0.10	0.031	31.4	16.4	25.8	26.4
1.40-0.10	0.011	10.7	17.2	27.4	44.7

Two pristine C-S-H's (C/S = 0.80 and 1.40) diffractograms are displayed (in black colour) in Figure 10. The typical C-S-H broad maxima are exhibited at small angles < 10° (2θ), and at ≈ 16.7, 29.1, 32.0, 49.8° (2θ) [26,32–34]. The sounds C-A-S-Hs' diffractograms (C/S = 0.80 and 1.40, Al/Si=0.05 and 0.1) shown in Figure 11 and Figure 12 displayed the same pattern as the C-S-H's but with broader peaks. One could attribute this feature to the presence of aluminium within the nanocrystalline C-S-H structure.

The <sup>29</sup>Si MAS-NMR spectra of the pristine and the carbonated C-S-H are displayed on Figure 5. One can see the alteration induced by the carbonation on C-S-H environments (Q<sup>1</sup>, Q<sup>2p</sup> and Q<sup>2b</sup>) leading to silica gel environment where higher silicates' coordination are predominant (Q<sup>3</sup> and Q<sup>4</sup>). The carbonation product was the same irrespective of the C/S ratios, i.e. a silica gel containing Q<sup>3</sup> and Q<sup>4</sup> environments. Two different C/S ratios are chosen to illustrate the observed C-A-S-H behavior upon carbonation: 0.8 and 1.2. The effect of carbonation on the C-A-S-H's lower C/S ratio 0.8, with an increasing aluminium contents, Al/Si = 0.05 and 0.1 is shown in Figure 6. The higher C/S ratio 1.2 at an Al/Si = 0.05 is presented on Figure 7. The carbonation product detected is the same as the one detailed previously for the C-S-H (silica gel with Q<sup>3</sup> and Q<sup>4</sup> environment). However, the silica gel environment incorporate a small fraction of silicates tetrahedra that are connected to two others tetrahedra (Q<sup>2</sup>), attributed to silicates tetrahedra with silanols as often observed in silica gel [24,29]. The estimated proportion of the Q<sup>2</sup> in the gel varies from 6 to 14 % for the C-A-S-H. The Q<sup>3</sup>/Q<sup>4</sup> ratio in the gel varies from 0.5 to 0.8 for all the C-A-S-Hs.

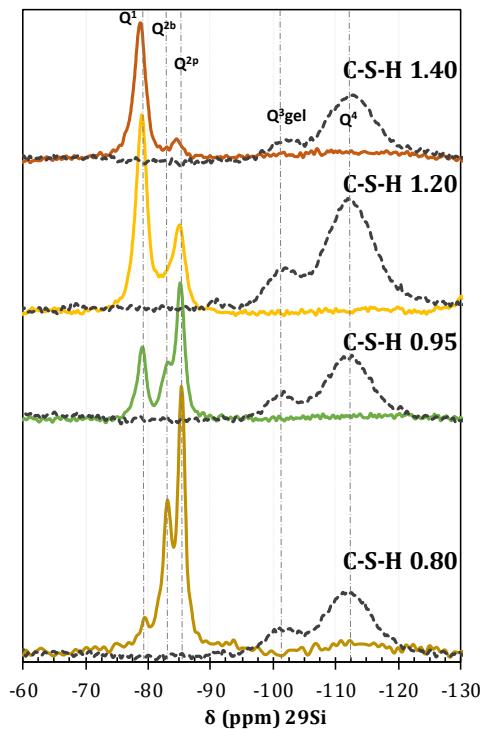


Figure 5:  $^{29}\text{Si}$  MAS NMR spectra of the non-carbonated (continued lines) and carbonated (dotted lines) C-S-H

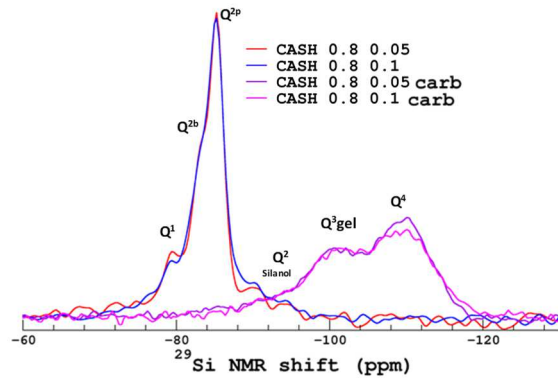


Figure 6:  $^{29}\text{Si}$  MAS NMR spectra of the non-carbonated and carbonated C-A-S-H ( $\text{Al/Si} = 0.05$ )

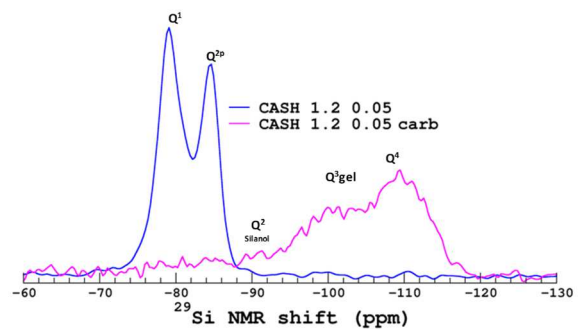
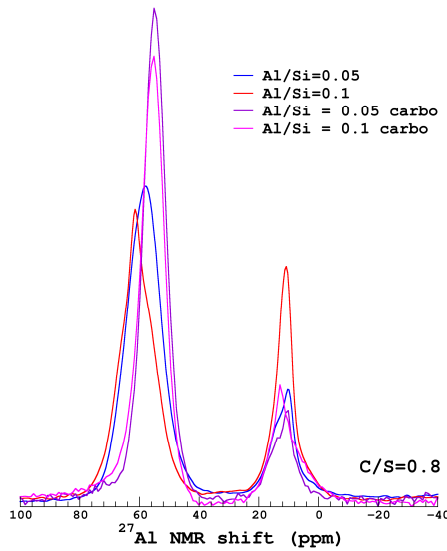
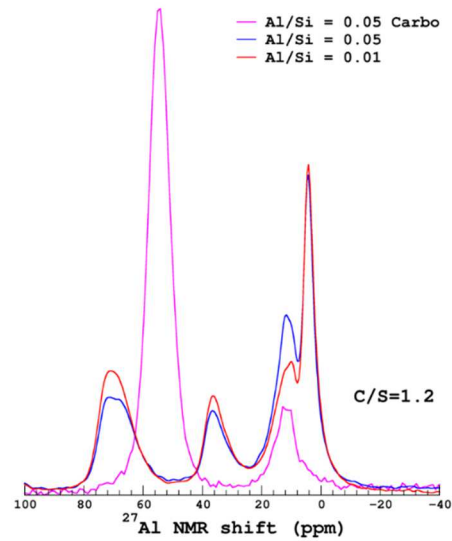


Figure 7 :  $^{29}\text{Si}$  MAS NMR spectra of the non-carbonated and carbonated C-A-S-H ( $\text{Al/Si} = 0.10$ )

The  $^{27}\text{Al}$  MAS-NMR spectra of both the carbonated and the pristine materials  $\text{C/S} = 0.80$ ,  $\text{Al/Si} = 0.05$  and  $0.10$  are displayed in Figure 8, the same features are shown for the C-A-S-H  $\text{C/S} = 1.20$   $\text{Al/Si} = 0.05$  in Figure 9. The spectra of the carbonation product exhibited the same type of environment for all calcium and Al contents. The calcium aluminate hydrate environment (around 10 ppm) was partially affected by the carbonation. The tetrahedral environments of the pristine material was altered by carbonation resulting in a silica gel embedding Ca and Al. Tetrahedral Al environment within the gel is observed at a lower resonance frequency compared to the pristine material. The carbonation of the C-A-S-H of  $\text{C/S} = 1.20$  gave insight on the change in all Al environment upon carbonation: another tetrahedral environment was produced; pentahedral environment and octahedral environment such as TAH were not observed after carbonation; their Al was mobilized into the newly formed tetrahedral environment. The resonances of calcium aluminates hydrate (Al h) that are not included in the C-A-S-H structure remained unchanged.



**Figure 8:**  $^{27}\text{Al}$  MAS NMR spectra of the pristine and carbonated C-A-S-H C/S= 0.80 Al/Si= 0.05; 0.10



**Figure 9:**  $^{27}\text{Al}$  MAS NMR spectra of pristine C-A-S-H C/S= 1.20 Al/Si= 0.05; 0.10 and the spectra of Al=0.05 carbonated material

The C-S-H diffractograms after accelerated and natural carbonation are presented on Figure 10. One can notice that vaterite was the main product, with aragonite as minor phase on either type of carbonation. After 18 days of accelerated carbonation, the typical C-S-H signal disappeared from the diffractograms of accelerated carbonation for all C/S ratios (1.40 and 0.80). The diffractograms of the C-A-S-Hs of Al/Si = 0.05 and Al/Si = 0.10 are displayed on Figure 11 and Figure 12 respectively. The C-A-S-Hs powders exhibited the same crystalline products as the C-S-H after carbonation, i.e. vaterite as the main phase and aragonite as minor phase. After 34 days of accelerated carbonation, the degradation of the C-A-S-H (Al/Si = 0.05 and 0.10) revealed to be incomplete for the higher C/S ratios (1.20 and 1.40) for which C-(A)-S-H signal was still detected. Conversely to C-S-H carbonation, which was complete in less than 20 days for all C/S ratios.

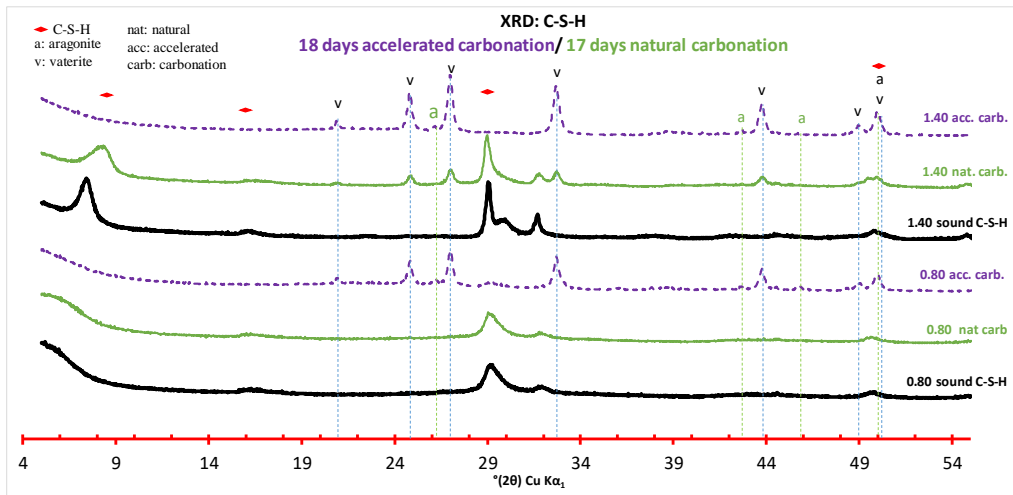


Figure 10: XRD of C-S-Hs' two C/S ratios 0.80 and 1.40, the pristine material (black), after 17 days of natural carbonation (green), and after 18 days of accelerated carbonation (purple)

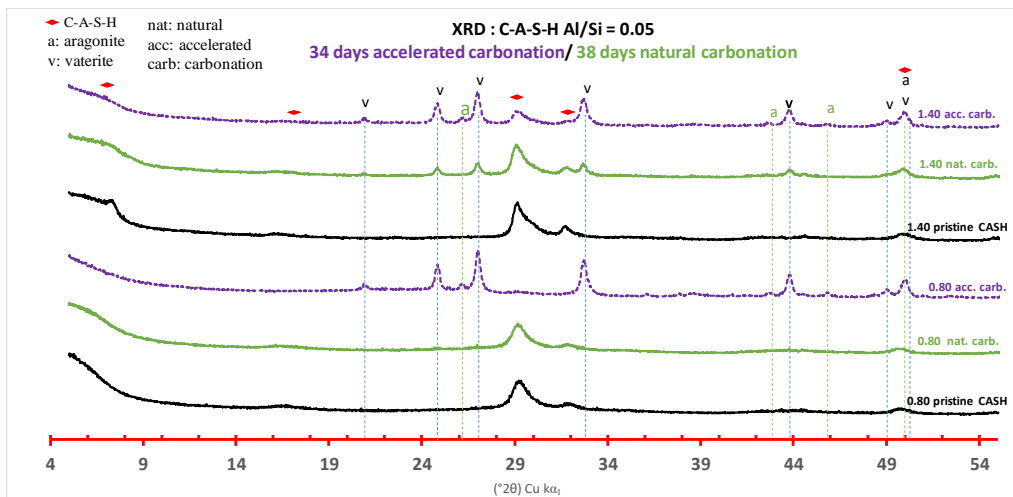


Figure 11: C-A-S-Hs XRD of C/S ratios 0.80 and 1.40 at an Al/Si = 0.05, the pristine material (black), after 38 days of nat. carbonation (green), and 34 days of acc. carbonation (purple)

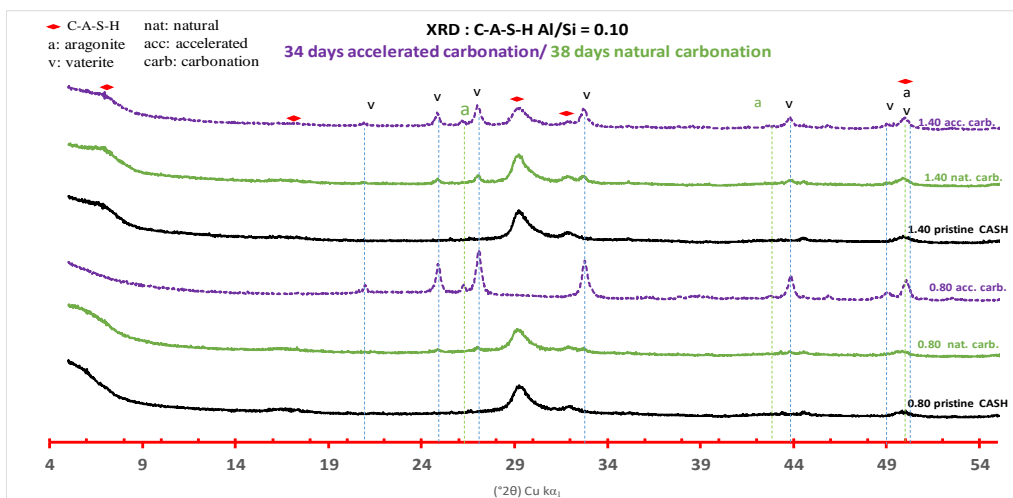
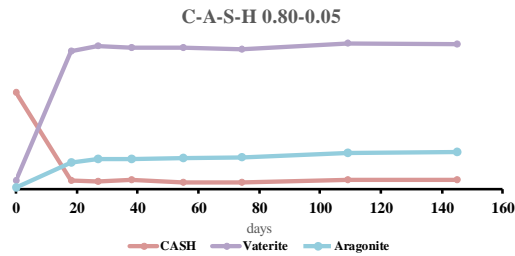
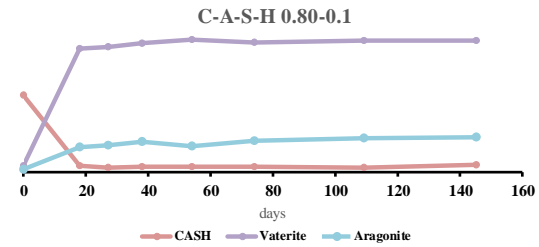


Figure 12: XRD of C-A-S-Hs C/S = 0.80 and 1.40 at an Al/Si= 0.1, pristine material (black), 38 days of nat. carbonation (green) and 34 days of acc. carbonation (purple)

The progress of the carbonation was monitored using XRD for C-A-S-Hs of C/S ratios of 0.80 and 1.40 and Al/Si ratios of 0.05 and 0.10. One can notice the complete carbonation of the C-A-S-H of low C/S ratio (0.80) in about 20 days regardless of the Al content (Figure 13 and Figure 14). The carbonation of higher C/S ratios (1.40 see Figure 15 and Figure 16) demonstrated reduced kinetics and incomplete carbonation after 145 days



**Figure 13: Progression of the C/S = 0.80 and Al/Si = 0.05 carbonated powder intensities (in arbitrary unit) with respect to time**



**Figure 14: Progression of the intensities (in arbitrary unit) of the phases observed during the carbonation of the C/S = 0.80 and Al/Si = 0.10 C-A-S-H, with respect to time.**

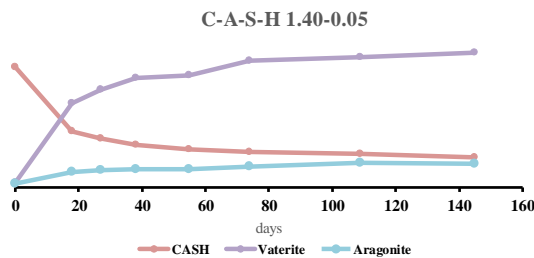


**Figure 15: Progression of the intensities (in arbitrary unit) of the phases observed during the carbonation of the C/S = 1.40 and Al/Si = 0.05 C-A-S-H, with respect to time.**

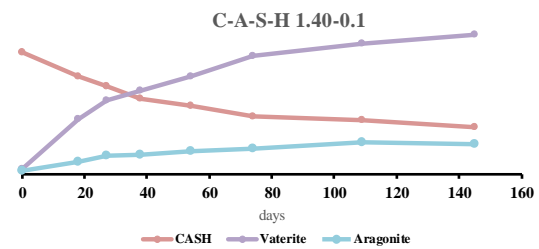


**Figure 16 : Progression of the intensities (in arbitrary unit) of the phases observed during the carbonation of the C/S = 1.40 and Al/Si = 0.10 C-A-S-H, with respect to time**

## 5. DISCUSSION

The  $^{29}\text{Si}$  MAS-NMR analyses evidenced the same (amorphous) carbonation end product for the C-A-S-H and C-S-H (a silica gel). However, in contrast to the case of C-S-H, the silica gel generated by the carbonation of the C-A-S-H evidenced a small fraction of  $\text{Q}^2$  silicates with a lower degree of coordination that we attributed to silanols. The presence of the silanols could be attributed to the presence of Al and Ca within the silica gel network. However, the  $\text{Q}^3/\text{Q}^4$  ratio in the gel for all the samples varied from 0.5 to 0.8. Similarly, the same (crystalline) carbonation products were evidenced by C-A-S-H and C-S-H, namely calcium carbonates. Two polymorphs were detected, a major and a minor phase, which were vaterite and aragonite respectively. For each sample, the progress of the carbonation was monitored using XRD. The C-S-H exhibited complete carbonation in about 20 days, regardless of the C/S ratio, likewise for the C-A-S-H samples of low C/S ratio (0.80). The carbonation of C-A-S-H samples with higher C/S ratios (especially 1.20 and 1.40) remained incomplete after 145 days of accelerated carbonation.

The effect of Al on C-S-H chemistry was studied using  $^{27}\text{Al}$  NMR. We focused on the changes related to Al environments following the carbonation. We observed the presence of pentahedral and octahedral (TAH) Al species prior to carbonation; those phases are known to occur at high calcium content in C-A-S-H interlayers and surfaces respectively. Those environments disappeared after carbonation. They were believed to slow down the C-A-S-H carbonation rate by limiting the access of the  $\text{CO}_2$ . Furthermore, the samples demonstrating the slower kinetics, incorporated the higher population of TAH and pentahedral Al environments. The incorporation of Al(IV) within the C-A-S-H appeared to have a

limited influence on the carbonation kinetics, since the low calcium samples C/S = 0.80 and 0.95 present the higher Al content of all the C-A-S-H tested in this study.

## 6. PRELIMINARY CONCLUSION

- Kinetics of degradation of C(-A)-S-Hs in materials submitted to carbonation is not based on the stability of the Si-O-Al bond, since there is no correlation observed between the Al (IV) content in C-A-S-H and the degradation kinetics.
- The main parameter seems to be the high calcium content which allows, in presence of Al, the formation of calcium aluminate species with aluminium in octahedral environment such as TAH and Al in pentahedral environment.
- There is a probable passivating effect of TAH and Al (V) calcium aluminates species leading to a limited CO<sub>2</sub> access to the C-A-S-H for high C/S ratios.

## 7. ACKNOWLEDGEMENTS

The financial support from IRSN and CEA is gratefully acknowledged.

## References

- [1] S. Goñi, M.T. Gaztañaga, a. Guerrero, Role of Cement Type on Carbonation Attack, *J. Mater. Res.* 17 (2002) 1834–1842. doi:10.1557/JMR.2002.0271.
- [2] V.T. Ngala, C.L. Page, Effects of carbonation on pore structure and diffusional properties of hydrated cement pastes, *Cem. Concr. Res.* 27 (1997) 995–1007.
- [3] Y.F. Houst, Y.F. Houst, F.H. Wittmann, F.H. Wittmann, Depth profiles of carbonates formed during natural carbonation, *Cem. Concr. Res.* 32 (2002) 1923–1930. doi:10.1016/s0008-8846(02)00908-0.
- [4] M. Thiery, G. Villain, P. Dangla, G. Platret, Investigation of the carbonation front shape on cementitious materials: Effects of the chemical kinetics, *Cem. Concr. Res.* 37 (2007) 1047–1058. doi:10.1016/j.cemconres.2007.04.002.
- [5] I. Monteiro, F.A. Branco, J. De Brito, R. Neves, Statistical analysis of the carbonation coefficient in open air concrete structures, *Constr. Build. Mater.* 29 (2012) 263–269. doi:10.1016/j.conbuildmat.2011.10.028.
- [6] F. Claret, S. Grangeon, A. Loschetter, C. Tournassat, W. De Nolf, N. Harker, F. Boulahya, S. Gaboreau, Y. Linard, X. Bourbon, A. Fernandez-Martinez, J. Wright, Deciphering mineralogical changes and carbonation development during hydration and ageing of a consolidated ternary blended cement paste, *IUCrJ.* 5 (2018) 150–157. doi:10.1107/S205225251701836X.
- [7] L. Black, C. Breen, J. Yarwood, K. Garbev, P. Stemmermann, B. Gasharova, Structural Features of C-S-H(I) and Its Carbonation in Air-A Raman Spectroscopic Study. Part II: Carbonated Phases, *J. Am. Ceram. Soc.* 90 (2007) 908–917. doi:10.1111/j.1551-2916.2006.01429.x.
- [8] E.G. Swenson, P.J. Sereda, Mechanism of the carbonation shrinkage of lime and hydrated cement, *J. Appl. Chem.* 18 (2007) 111–117. doi:10.1002/jctb.5010180404.
- [9] K. Kamimura, P.J. Sereda, E.G. Swenson, Changes in weight and dimensions in the drying and carbonation of Portland cement mortars, *Mag. Concr. Res.* 17 (1965) 5–14.
- [10] E.G. Swenson, P.J. Sereda, Mechanism of the carbonation shrinkage of lime and hydrated cement, *J. Appl. Chem.* 18 (1968) 111–117.
- [11] M. Auroy, S. Poyet, P. Le Bescop, J.M. Torrenti, T. Charpentier, M. Moskura, X. Bourbon, Impact

- of carbonation on unsaturated water transport properties of cement-based materials, *Cem. Concr. Res.* 74 (2015) 44–58. doi:10.1016/j.cemconres.2015.04.002.
- [12] M. Auroy, S. Poyet, P. Le Bescop, J.-M. Torrenti, T. Charpentier, M. Moskura, X. Bourbon, Comparison between natural and accelerated carbonation (3% CO<sub>2</sub>): Impact on mineralogy, microstructure, water retention and cracking, *Cem. Concr. Res.* 109 (2018) 64–80. doi:10.1016/j.cemconres.2018.04.012.
- [13] E. Drouet, S. Poyet, P. Le Bescop, J.-M. Torrenti, X. Bourbon, Carbonation of hardened cement pastes: Influence of temperature, *Cem. Concr. Res.* 115 (2019) 445–459. doi:10.1016/j.cemconres.2018.09.019.
- [14] G.W. Groves, D.I. Rodway, I.G. Richardson, The carbonation of hardened cement pastes, *Adv. Cem. Res.* 3 (1990) 117–125.
- [15] G.W. Groves, A. Brough, I.G. Richardson, C.M. Dobson, Progressive changes in the structure of hardened C3S cement pastes due to carbonation, *J. Am. Ceram. Soc.* 74 (1991) 2891–2896.
- [16] A. Silva, R. Neves, J. De Brito, Statistical modelling of carbonation in reinforced concrete, *Cem. Concr. Compos.* 50 (2014) 73–81. doi:10.1016/j.cemconcomp.2013.12.001.
- [17] J. Chang, Y. Fang, Quantitative analysis of accelerated carbonation products of the synthetic calcium silicate hydrate(C-S-H) by QXRD and TG/MS, *J. Therm. Anal. Calorim.* 119 (2015) 57–62. doi:10.1007/s10973-014-4093-8.
- [18] A. Dauzeres, P. Le Bescop, P. Sardini, C. Cau Dit Coumes, Physico-chemical investigation of clayey/cement-based materials interaction in the context of geological waste disposal: Experimental approach and results, *Cem. Concr. Res.* 40 (2010) 1327–1340. doi:10.1016/j.cemconres.2010.03.015.
- [19] F. Brunet, T. Charpentier, C.N. Chao, H. Peycelon, A. Nonat, Characterization by solid-state NMR and selective dissolution techniques of anhydrous and hydrated CEM V cement pastes, *Cem. Concr. Res.* 40 (2010) 208–219. doi:10.1016/j.cemconres.2009.10.005.
- [20] F. Brunet, P. Bertani, T. Charpentier, A. Nonat, J. Virlet, Application of <sup>29</sup>Si Homonuclear and <sup>1</sup>H-<sup>29</sup>Si Heteronuclear NMR Correlation to Structural Studies of Calcium Silicate Hydrates, *J. Phys. Chem. B* . 108 (2004) 15494–15502. doi:10.1021/jp031174g.
- [21] X. Cong, R. James Kirkpatrick, <sup>17</sup>O and <sup>29</sup>Si MAS NMR study of β-C<sub>2</sub>S hydration and the structure of calcium-silicate hydrates, *Cem. Concr. Res.* 23 (1993) 1065–1077. doi:10.1016/0008-8846(93)90166-7.
- [22] J.J. Chen, J.J. Thomas, H.F.W. Taylor, H.M. Jennings, Solubility and structure of calcium silicate hydrate, *Cem. Concr. Res.* 34 (2004) 1499–1519. doi:10.1016/j.cemconres.2004.04.034.
- [23] P. Faucon, A. Delagrave, J.C. Petit, C. Richet, J.M. Marchand, H. Zanni, Aluminum Incorporation in Calcium Silicate Hydrates (C-S-H) Depending on Their Ca/Si Ratio, *J. Phys. Chem. B*. 103 (1999) 7796–7802. doi:10.1021/jp990609q.
- [24] G.K. Sun, J.F. Young, R.J. Kirkpatrick, The role of Al in C-S-H: NMR, XRD, and compositional results for precipitated samples, *Cem. Concr. Res.* 36 (2006) 18–29. doi:10.1016/j.cemconres.2005.03.002.
- [25] E. L'Hôpital, B. Lothenbach, D.A. Kulik, K. Scrivener, Influence of calcium to silica ratio on aluminium uptake in calcium silicate hydrate, *Cem. Concr. Res.* 85 (2016) 111–121. doi:10.1016/j.cemconres.2016.01.014.
- [26] C. Roos, P. Vieillard, P. Blanc, S. Gaboreau, H. Gailhanou, D. Braithwaite, V. Montouillout, R.

- Denoyel, P. Henocq, B. Madé, Thermodynamic properties of C-S-H, C-A-S-H and M-S-H phases: Results from direct measurements and predictive modelling, *Appl. Geochemistry*. 92 (2018) 140–156. doi:10.1016/j.apgeochem.2018.03.004.
- [27] D. Müller, W. Gessner, H.J. Behrens, G. Scheler, Determination of the aluminium coordination in aluminium-oxygen compounds by solid-state high-resolution  $^{27}\text{Al}$  NMR, *Chem. Phys. Lett.* 79 (1981) 59–62. doi:10.1016/0009-2614(81)85288-8.
- [28] P. Faucon, T. Charpentier, D. Bertrandie, a. Nonat, J. Virlet, J.C. Petit, Characterization of Calcium Aluminate Hydrates and Related Hydrates of Cement Pastes by  $(^{27}\text{Al})$  MQ-MAS NMR., *NMR Cem. No. 37* (1998) 3726–3733. doi:10.1021/ic9800076.
- [29] T.F. Sevelsted, J. Skibsted, Carbonation of C-S-H and C-A-S-H samples studied by  $^{13}\text{C}$ ,  $^{27}\text{Al}$  and  $^{29}\text{Si}$  MAS NMR spectroscopy, *Cem. Concr. Res.* 71 (2015) 56–65. doi:10.1016/j.cemconres.2015.01.019.
- [30] E. Kapeluszna, Ł. Kotwica, A. Różycka, Ł. Gołek, Incorporation of Al in C-A-S-H gels with various Ca/Si and Al/Si ratio: Microstructural and structural characteristics with DTA/TG, XRD, FTIR and TEM analysis, *Constr. Build. Mater.* 155 (2017) 643–653. doi:10.1016/j.conbuildmat.2017.08.091.
- [31] M.D. Andersen, H.J. Jakobsen, J. Skibsted, A new aluminium-hydrate species in hydrated Portland cements characterized by  $^{27}\text{Al}$  and  $^{29}\text{Si}$  MAS NMR spectroscopy, *Cem. Concr. Res.* 36 (2006) 3–17. doi:10.1016/j.cemconres.2005.04.010.
- [32] K. Garbev, G. Beuchle, M. Bornefeld, L. Black, P. Stemmermann, Cell dimensions and composition of nanocrystalline calcium silicate hydrate solid solutions. Part 1: synchrotron-based x-ray diffraction, *J. Am. Ceram. Soc.* 91 (2008) 3005–3014. doi:10.1111/j.1551-2916.2008.02484.x.
- [33] S. Grangeon, F. Claret, C. Lerouge, F. Warmont, T. Sato, S. Anraku, C. Numako, Y. Linard, B. Lanson, On the nature of structural disorder in calcium silicate hydrates with a calcium/silicon ratio similar to tobermorite, *Cem. Concr. Res.* 52 (2013) 31–37. doi:10.1016/j.cemconres.2013.05.007.
- [34] I.G. Richardson, Model structures for C-(A)-S-H(I), *Acta Crystallogr. Sect. B Struct. Sci. Cryst. Eng. Mater.* 70 (2014) 903–923. doi:10.1107/S2052520614021982.